

Temperature distribution in poly(ethylene terephthalate) plate undergoing heat treatment. Diffusion influence:

1. Theoretical approach

Ph. Lebaudy*, J. M. Saiter, J. Grenet and C. Vautier

L.E.C.A.P., Faculté des Sciences de Rouen, BP 118,

76134 Mont-Saint-Aignan Cedex, France

(Received 28 September 1990; revised 5 March 1991; accepted 5 June 1991)

A model is developed in order to calculate temperature distributions in polymer plates undergoing heat treatment. The model takes into account the scattering of the medium. Some examples are presented that illustrate the differences in the behaviour of glassy and crystalline PET plates subjected to the same heat treatment.

(Keywords: poly(ethylene terephthalate); scattering; temperature effect)

INTRODUCTION

A knowledge of temperature distributions in a polymeric medium undergoing various heat treatments is of fundamental importance in forming processes¹. Indeed, visco-elastic properties and crystallization kinetics depend on the temperature. Heating by means of infrared radiation is particularly used in thermoforming². Such heating has a great advantage over heating processes based on heat conduction or convection: part of the energy directly penetrates the interior of the semi-finished thermoplastic product and thus is not subject to the slow heat conduction process which characterizes plastics (for example, the thermal conductivity is only $0.29 \text{ W m}^{-1} \text{ K}^{-1}$ for PETP, in contrast to $400 \text{ W m}^{-1} \text{ K}^{-1}$ for copper)³. However, experimental measurements are not readily practicable, and usually computation is used to determine the temperature distribution in sheets of diathermanous materials⁴. In methods of computation previously used, all the models are based on the equation for unidimensional unsteady-state heat conduction with a location-dependent heat source^{5,6}. This heat source takes into account the spectral absorption at different layer depths in the material and the spectral emission of the radiator.

When the polymeric medium is a semi-crystalline polymer or when impurities are present in the polymer, scattering may occur during heat treatment. The radiative heat transfer modification induced by this spectral scattering of the medium changes the temperature distribution inside the material. The impurities or the crystalline structures (called spherulites) have a different refractive index from that of the matrix and therefore induce light-scattering⁷. For a semi-crystalline polymer the size and number of spherulites are generally determined by the thermal history of the material. Consequently, if

during the thermal process the polymer goes through the crystallization temperature range, the size and number of spherulites as well as the spectral scattering parameters change⁸.

The aim of the present work was to construct a model which takes into account the influence of this spectral scattering parameter on the temperature distribution inside a material undergoing heat treatment. A comparison between numerical and experimental results on PET plates will be presented in Part 2, subtitled Applications.

MATERIALS AND INFRARED INTERACTIONS

Generally, in plastics processing, quartz radiators are used as infrared radiation sources. These radiators can be used in the temperature range 1000 to 2500 K. A change in temperature leads to a change in the distribution of the radiation intensity with wavelength. For a black body, the intensity of radiation emitted into a hemisphere is described by the Planck law and, according to the Stefan-Boltzmann law, the total energy emitted into this hemisphere is given by $q = \sigma_s T^4$, where σ_s is the Stefan constant, while the variation of emitted energy with wavelength is obtained by integration of the Planck law. For a real radiator the effective energy emitted is smaller than that of an ideal black body through the value of the emissivity ϵ_λ . Moreover, the transmittance and the emissivity of the protective quartz envelope of the metallic filament have to be taken into account. Because these parameters are not easy to determine theoretically, the irradiance of the complete radiator has been measured in this work (Figure 1). Owing to the emissivity of the protective quartz envelope

* To whom correspondence should be addressed

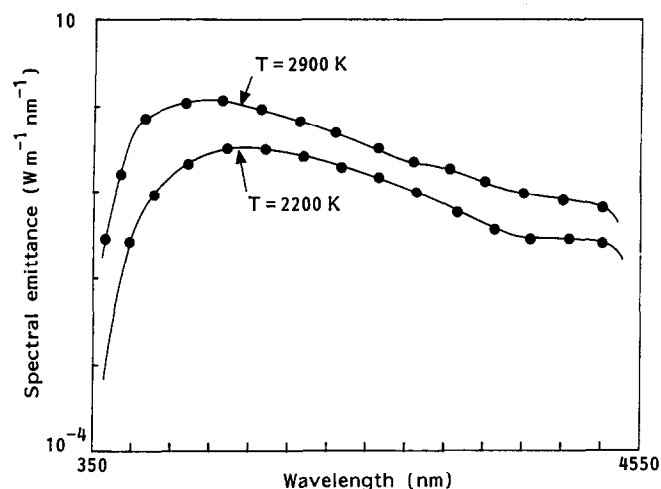


Figure 1 Spectral emittance of radiation versus wavelength at two temperatures; the peak around 2 μm and the slight elevation around 4 μm are due to the filament and the quartz envelope spectral emittance respectively

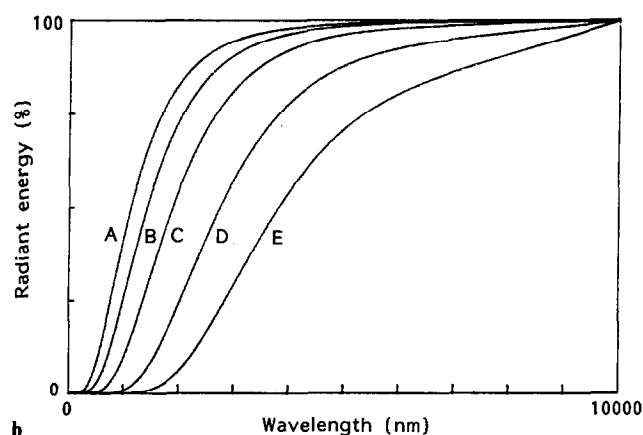
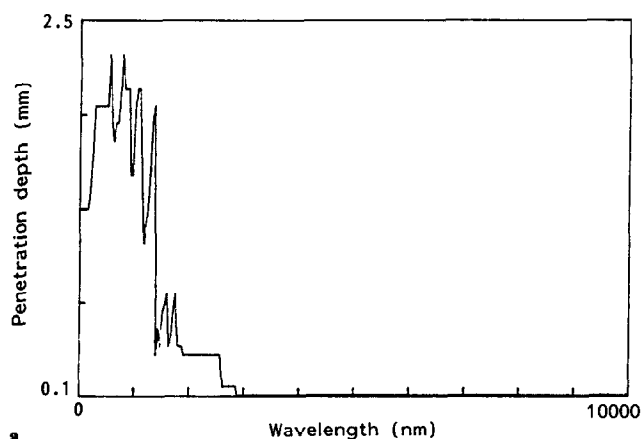


Figure 2 (a) Penetration depth versus wavelength for a PET film. (b) Total energy emitted versus wavelength for different radiator temperatures: a, 2500 K; b, 2000 K; c, 1500 K; d, 1000 K; e, 700 K

(the temperature of which is about 1000 K), the spectral response of the radiator shows a slight elevation.

The absorptivity A_λ , the reflectance R_λ , the transmittance T_λ , and the scattering factor σ_λ are linked by:

$$A_\lambda + R_\lambda + T_\lambda + \sigma_\lambda = 1 \quad (1)$$

These coefficients are well known to be wavelength-dependent, so a knowledge of their spectral response is of great importance.

In order to describe the spectral absorption characteristics of the material, the Lambert–Bouguer law is used here. For practical considerations, it was found to be advantageous to describe the absorption behaviour in terms of penetration depth E_λ , the reciprocal of the absorption coefficient. The radiation intensity at point x is given by

$$I(x) = I_0 \exp(-x/E_\lambda) \quad (2)$$

where I_0 is the radiation intensity at $x = 0$, and E_λ the spectral penetration depth.

The variations of penetration depth with wavelength for a glassy poly(ethylene terephthalate) (PET) sample are reported in Figure 2. It may be noticed that the material absorbs slightly in the visible and near-infrared regions, and strongly in the far-infrared region. This behaviour is not a particularity of PET but a common feature of the absorption spectrum of polymers because of similarities in their chemical structures.

At the interface between materials differing in optical density, a fraction of the incident radiation penetrates into the material, while a fraction is reflected. This reflected fraction is relatively low, generally 4–5% of the incident flux, even for glossy surfaces⁹. For a thin film, the actual reflectance can be twofold, because the reflection occurring when the beam goes through the back of the plate must be added to the front surface reflection. In this case the losses by reflection and absorption may be equal.

In a scattering medium, the assumption that the path of the radiation beam through the material is rectilinear is no longer justified, and then it is not possible to use the Lambert–Bouguer law to describe the radiative flux behaviour. Therefore in order to calculate this radiative flux, a four-flux model has been used. The spectral scattering coefficient σ_λ required for this calculation of glassy and crystallized PET is given by $\sigma_\lambda = W_\lambda K_\lambda / (1 - W_\lambda)$, where K_λ is the absorption coefficient and W_λ the albedo. The measurement of this albedo has been performed with a spectrometer equipped with a globe photometer. Experimental results, reported in Figure 3, show that this parameter is highly dependent on wavelength and on the crystallinity of the polymer. As it is not easy to obtain samples of given crystalline fractions experimentally, and therefore to determine their respective spectral scattering coefficients, it has been assumed that the variation of the spectral scattering coefficient with crystalline fraction is linear.

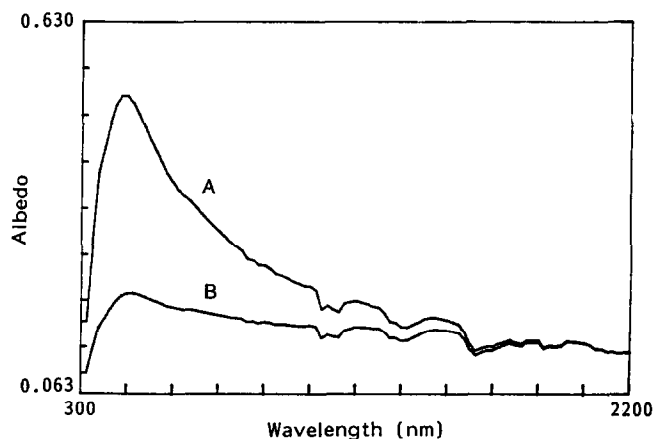


Figure 3 Scattering coefficient versus wavelength for (A) crystallized PET, (B) glassy PET

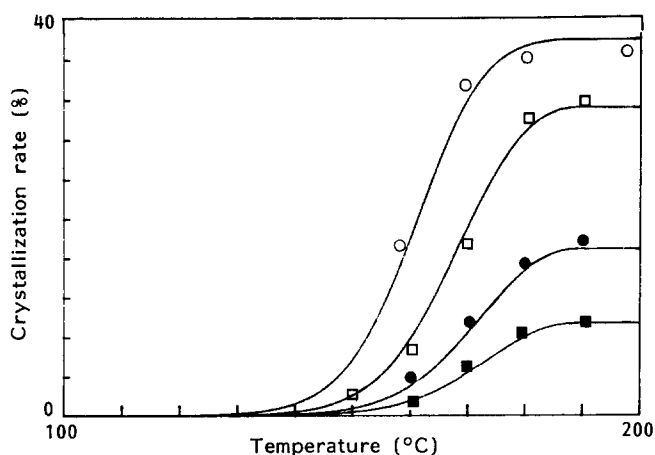


Figure 4 Crystalline fraction versus temperature for different heating rates; experimental points obtained by d.s.c., and corresponding curves determined by equation (4). \circ , $v = 5^\circ\text{C min}^{-1}$; \square , $v = 10^\circ\text{C min}^{-1}$; \bullet , $v = 20^\circ\text{C min}^{-1}$; \blacksquare , $v = 25^\circ\text{C min}^{-1}$

The crystalline fraction is calculated using Ozawa's theory¹⁰, which is suitable for describing the crystallization kinetics of the material when the process proceeds under non-isothermal conditions and when the cooling rate or the heating rate changes. In this treatment, which extends Avrami and Evans's isothermal theory¹¹⁻¹⁴, the transformed fraction $\alpha(T)$, at temperature T and for a cooling (or heating) rate v , is given by

$$\alpha(T) = 1 - \exp[-\chi(T)/|v|^n] \quad (3)$$

where $\chi(T)$ is the heating (or cooling) crystallization function of the polymer, and n is the Avrami number. If the cooling or heating rate changes during the process, the transformed fraction is obtained by¹⁵:

$$\alpha(T_p) = 1 - \exp\left[-\left(\sum_{i=1}^p \left|\frac{\chi^{1/n}(T_i) - \chi^{1/n}(T_{i-1})}{v_i}\right|\right)^n\right] \quad (4)$$

The heating crystallization function of the polymer and Avrami number were determined by means of thermal analysis, using a d.s.c. analyser¹⁶. Figure 4 shows the curves calculated, using Ozawa's theory, from the experimental data. Following Deterre¹⁷, the maximum crystallization rate is never higher than 40% for PET.

Given the spectral dependence of the various parameters—emission of the radiator, absorption of the medium, reflection, scattering of the medium—the heating problem can now be analysed.

THE HEATING PROBLEM

The experimental results reported in Figure 2b show that a radiator at a temperature of 1000 K emits 75% of its energy between 3 and 10 μm , whereas only 30% of the radiation energy of a radiator at a temperature of 2500 K lies in the high-absorption region of PET. In the first case, it is possible to consider that the total energy, except that reflected at the surface, is absorbed. Despite optimal energy efficiency, this heating method is not always advantageous, especially for thick plates, because of the marked absorption by the surface layers. Moreover, the heating rate is governed by the very slow heat conduction process, which leads to high temperature gradients. In the second case, a fraction of the energy is

absorbed in the interior of the material, leading to a spontaneous increase in temperature, but a large fraction of the radiation passes through the material and is wasted. It is obvious that the objectives of temperature uniformity and energy efficiency conflict with one another.

The usual mechanisms of heat transfer¹⁸ are outside the scope of this paper. Here we consider, for the sake of simplicity, the equation for unidimensional unsteady-state heat conduction with two location-dependent heat sources¹⁹:

$$\frac{\delta^2 T}{\delta x^2} - \frac{1}{a} \frac{\delta T}{\delta \tau} + \frac{S(x)}{k} + \frac{\Delta H_c}{aC_p} \frac{\delta \alpha(x)}{\delta \tau(x)} = 0 \quad (5)$$

where T is the temperature, τ the time, k the thermal conductivity, a the thermal diffusivity, x the depth, $S(x)/k$ the first location-dependent heat source, which corresponds to the infrared absorption, and

$$\frac{\Delta H_c}{aC_p} \frac{\delta \alpha(x)}{\delta \tau(x)}$$

the second location-dependent heat source, induced by the material crystallization enthalpy, where ΔH_c is the crystallization enthalpy, C_p the specific heat capacity, and $\delta \alpha(x)/\delta \tau(x)$ the evolution of the transformed fraction.

CRYSTALLIZATION ENTHALPY HEAT SOURCE

This heat source is taken into account only when the material goes through the crystallization temperature range. In this case, the measurement of the evolution of the transformed fraction $\delta \alpha/\delta \tau$ (calculated by Ozawa's equation) gives the value of the source. For PET the temperature rise induced by this heat source may vary from 0 to 20°C, depending on the crystallization rate.

THE HEAT SOURCE TRANSFER EQUATION $S(x)$

The heat source induced by i.r. absorption is highly dependent on the optical properties of the material^{19,20}. These properties are characterized^{21,22} by the absorption coefficient K_λ , the scattering coefficient σ_λ , and the scattering phase function P_λ . Taking L as the irradiance, the general form of the transfer equation is

$$\frac{dL}{dx} = -K_\lambda L_\lambda - \sigma_\lambda L_\lambda + K_\lambda L_\lambda^0 T + \frac{\sigma_\lambda}{4\pi} \int P_\lambda(x, \Omega', \Omega) L d\Omega' \quad (6)$$

where the first and second terms correspond to the losses of irradiance by absorption and scattering respectively. The third term is the intrinsic emission of the polymer at temperature T (which in the present case could be neglected). The last term is the increase in irradiance induced by light-scattering in the direction considered. The scattering phase function $P_\lambda(x, \Omega', \Omega)$ is the ratio of the value of scattering irradiance in one direction (Ω) to the value of this scattering irradiance for an isotropic scattering medium. In order to determine the phase function, the Schuster-Schwarzschild approximation²³ has been used, which supposes that irradiance is isotropic

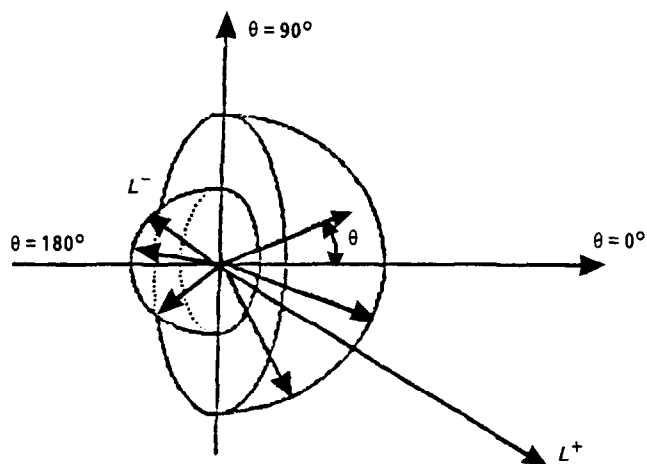


Figure 5 Illustration of Schuster-Schwarzschild approximation

for each hemisphere (Figure 5). Then the heat transfer equation becomes

$$\frac{\partial L_{\lambda}^{-}}{\partial x} - (2K_{\lambda} + \sigma_{\lambda})L_{\lambda}^{-} + \sigma_{\lambda}L_{\lambda}^{+} = 0 \quad (7)$$

$$\frac{\partial L_{\lambda}^{+}}{\partial x} + (2K_{\lambda} + \sigma_{\lambda})L_{\lambda}^{+} - \sigma_{\lambda}L_{\lambda}^{-} = 0 \quad (8)$$

As the radiation is directional, we cannot consider the induced irradiance as isotropic. Then it is necessary to add a collimated flux to the isotropic irradiance. These collimated fluxes I_{λ}^{+} and I_{λ}^{-} and the isotropic irradiances L_{λ}^{+} and L_{λ}^{-} lead to a four-flux model^{24,25}:

$$\frac{\partial I_{\lambda}^{-}}{\partial x} - K_{\lambda}I_{\lambda}^{-} - \sigma_{\lambda r}I_{\lambda}^{-} - \sigma_{\lambda t}I_{\lambda}^{-} = 0 \quad (9a)$$

$$\frac{\partial I_{\lambda}^{+}}{\partial x} - K_{\lambda}I_{\lambda}^{+} - \sigma_{\lambda r}I_{\lambda}^{+} - \sigma_{\lambda t}I_{\lambda}^{+} = 0 \quad (9b)$$

$$\frac{\partial L_{\lambda}^{-}}{\partial x} - 2(K_{\lambda} + \sigma_{\lambda r})L_{\lambda}^{-} + 2\sigma_{\lambda r}L_{\lambda}^{+} = -(\sigma_{\lambda r}I_{\lambda}^{+} + \sigma_{\lambda t}I_{\lambda}^{-})/\pi \quad (9c)$$

$$\frac{\partial L_{\lambda}^{+}}{\partial x} - 2(K_{\lambda} + \sigma_{\lambda r})L_{\lambda}^{+} + 2\sigma_{\lambda r}L_{\lambda}^{-} = -(\sigma_{\lambda r}I_{\lambda}^{+} + \sigma_{\lambda t}I_{\lambda}^{-})/\pi \quad (9d)$$

where $\sigma_{\lambda t}$ is the transmission scattering coefficient and $\sigma_{\lambda r}$ the reflection scattering coefficient.

This system leads to

$$I_{\lambda}^{-} = I_{m\lambda} \exp(\beta_{\lambda}x) \quad (10a)$$

$$I_{\lambda}^{+} = I_{p\lambda} \exp(-\beta_{\lambda}x) \quad (10b)$$

$$L_{\lambda}^{-} = a_{\lambda}^{-} \exp(-\gamma_{\lambda}x) + b_{\lambda}^{-} \exp(\gamma_{\lambda}x) + c_{\lambda}^{-} \exp(-\beta_{\lambda}x) + d_{\lambda}^{-} \exp(\beta_{\lambda}x) \quad (10c)$$

$$L_{\lambda}^{+} = a_{\lambda}^{+} \exp(-\gamma_{\lambda}x) + b_{\lambda}^{+} \exp(\gamma_{\lambda}x) + c_{\lambda}^{+} \exp(-\beta_{\lambda}x) + d_{\lambda}^{+} \exp(\beta_{\lambda}x) \quad (10d)$$

where

$$\gamma_{\lambda} = 2[K_{\lambda}(K_{\lambda} + \sigma_{\lambda t} + \sigma_{\lambda r})]^{1/2}$$

and $\beta_{\lambda} = (K_{\lambda} + \sigma_{\lambda t} + \sigma_{\lambda r})$ is the extinction coefficient.

The spectral radiative flux is the summation of the two fluxes and the two irradiances:

$$\Phi_{\lambda}(x) = (I_{\lambda}^{+} - I_{\lambda}^{-}) + \pi(L_{\lambda}^{+} - L_{\lambda}^{-}) \quad (11)$$

The spectral heat source $S_{\lambda}(x)$ is the divergence of the spectral radiative flux:

$$S_{\lambda}(x) = -\frac{d\Phi_{\lambda}(x)}{dx} = -\frac{d[(I_{\lambda}^{+} - I_{\lambda}^{-}) + \pi(L_{\lambda}^{+} - L_{\lambda}^{-})]}{dx} \quad (12)$$

The heat source $S(x)$ is then

$$S(x) = \int_{\lambda_1}^{\lambda_2} S_{\lambda}(x) d\lambda \quad (13)$$

where $\lambda_1 = 0.5\lambda_{max}$ and $\lambda_2 = 5\lambda_{max}$. This wavelength interval corresponds to 90% of the total energy emitted by the radiator⁹; λ_{max} is given by the Wien law.

The variations of $S(x)$ with depth for glassy and for crystalline materials are shown, for $T = 2000$ K, in Figure 6. This figure shows that when the radiator temperature is high, the scattering influence on the heat transfer behaviour is preponderant.

This expression for $S(x)$, when introduced into equation (5), leads to a unidimensional unsteady-state heat conduction equation which has no analytical solutions. A computing program using finite differences has been developed for the selection of suitable i.r. radiator systems. Application of this program is now illustrated by calculations of the time and space dependence of temperature in PET plates undergoing various heat treatments.

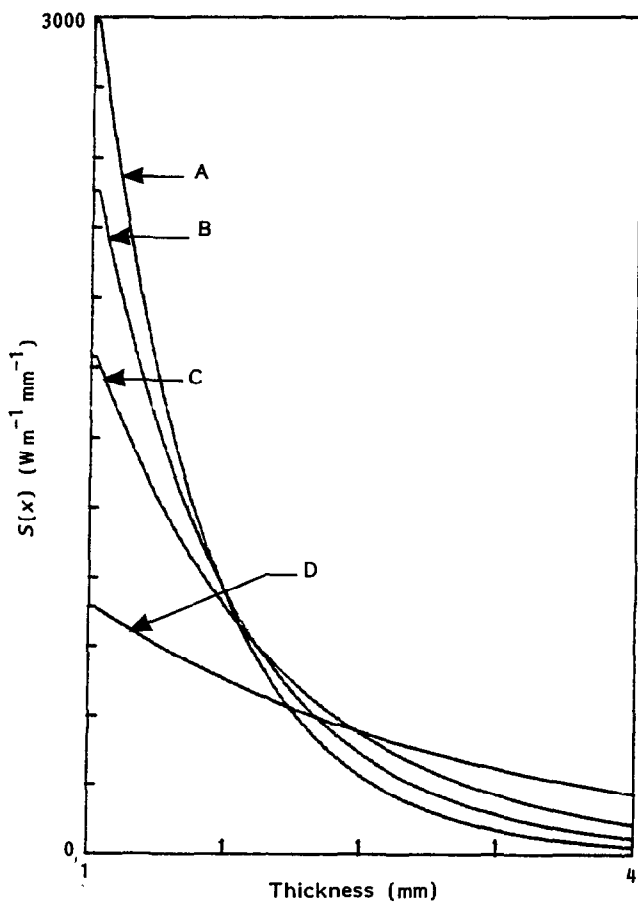


Figure 6 Heat source versus depth of crystalline and vitreous PET for two radiator temperatures: (A) crystalline, $T = 2000$ K; (B) vitreous, $T = 2000$ K; (C) crystalline, $T = 1000$ K; (D) vitreous, $T = 1000$ K

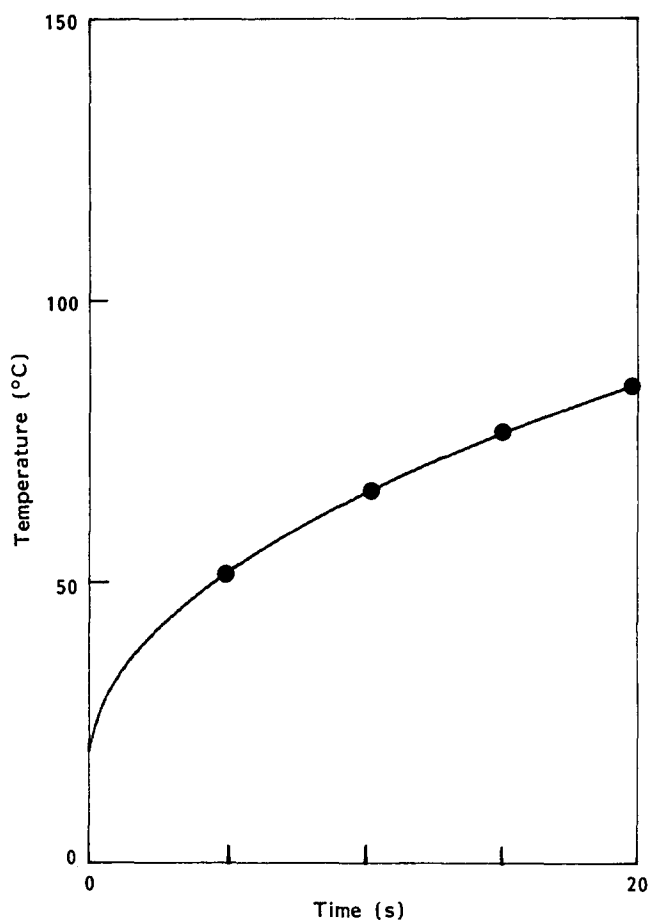


Figure 7 Surface temperature of PET plate versus time: experimental points and calculated curve

RESULTS

To check the validity of the simulation calculation, the surface temperatures of PET plates were measured with an i.r. camera after different heating times and compared with the numerical values. Figure 7 shows that good agreement was obtained between measured and calculated data.

Figure 8 shows the influence of radiator temperature and crystalline structure of the material on the temperature profile. All the simulations were done, for best understanding of the phenomenon, with a surface heat transfer coefficient equal to $50 \text{ W m}^{-2} \text{ K}^{-1}$. Comparison between curves A and C in Figure 8 confirms that a low radiator temperature improves the heating yield but leads to high temperature gradients. Curves A, B, C and D show that the thermal transfer modifications induced by scattering are more significant when the radiator temperature is high. Effectively, for the low-temperature radiator, the radiation absorption occurs principally at the surface of the material, whatever the structure of the material.

CONCLUSIONS

The heating of thick pieces or plates of polymer needs a high-temperature radiator, i.e. short-wave radiation. Such radiation is uniformly absorbed inside the medium and produces the uniform and rapid heating generally necessary in the forming process. Under these conditions, scattering in the material appreciably modifies the radiative heat transfer, and it is of prime necessity to

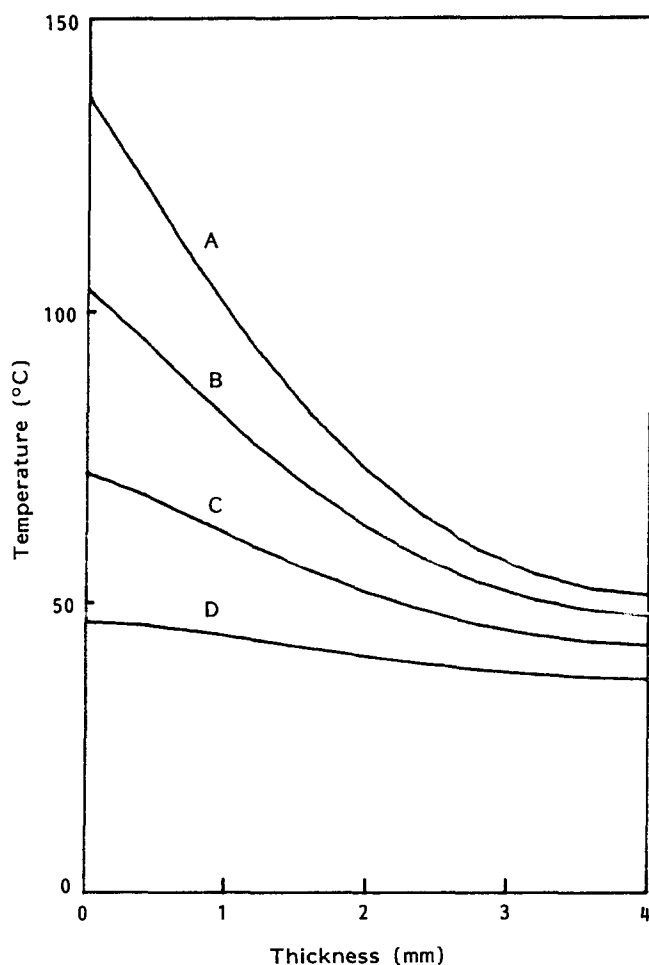


Figure 8 Temperatures profile with depth in crystalline and vitreous PET for two radiator temperatures: (A)–(D) as in Figure 6

take into account this phenomenon for optimization of heating. On the other hand, low-temperature radiators are used for heating thin sheets of polymer. In this case, the radiation absorption occurs exclusively at the surfaces of the sheet; consequently the modification of the optical properties induced by scattering does not change the radiative heat transfer and may be neglected. The influence of other parameters on the temperature distribution, such as the velocity and temperature of air blown over the plate surface during heating, will be discussed in Part 2, subtitled Applications.

REFERENCES

- 1 Progelhof, R. C., Quintiere, J. and Throne, J. L. *J. Appl. Polym. Sci.* 1971, **15**, 1803
- 2 Lunka, H. A. *SPE J.* 1970, **26**, 48
- 3 Martinet, J. 'Thermocinetique', Technique et Documentation, Paris, 1989
- 4 Cardon, R. *J. Am. Ceram. Soc.* 1958, **41**, 200
- 5 Lick, W. J. *Heat Mass Transfer* 1965, **8**, 119
- 6 Esser, K., Haberstroh, E., Hüsgen, U. and Weinand, D. *Adv. Polym. Technol.* 1987, **7**, 89
- 7 Haudin, J. M. 'Optical Properties of Polymers', Elsevier Applied Science Publishers, New York, 1986
- 8 Eckert, E. R. G. 'Analysis of Heat and Mass Transfer', McGraw-Hill, New York, 1972
- 9 Siegel and Howell. 'Thermal Radiation Heat Transfer', McGraw-Hill, New York, 1972
- 10 Ozawa, T. *Polymer* 1971, **12**, 150
- 11 Avrami, M. *J. Chem. Phys.* 1939, **7**, 1103
- 12 Avrami, M. *J. Chem. Phys.* 1940, **8**, 212
- 13 Avrami, M. *J. Chem. Phys.* 1941, **9**, 177
- 14 Evans, U. R. *Trans. Faraday Soc.* 1945, **41**, 365

Temperature distribution in PET plate undergoing heat treatment. 1: Ph. Lebaudy et al.

- 15 Billon, N. Thesis, Ecole des Mines, Paris, 1987
- 16 Lebaudy, Ph. Thesis, Rouen, 1989
- 17 Deterre, R. Thesis, Strasbourg, 1984
- 18 Carslaw, H. S. and Jaeger, J. C. 'Conduction of Heat in Solids', Oxford, Science Publications, 1959
- 19 Taine, J. in 'Transferts Thermiques Couplés: Colloque de Thermique des Systèmes et des Procédés', C.N.R.S., Paris, 1988
- 20 Lallemand, M. and Sacadura, J. F. in 'Transferts Thermiques Couplés: Colloque de Thermique des Systèmes et des Procédés', C.N.R.S., Paris, 1988
- 21 Devriendt, A. B. 'La Transmission de la Chaleur', Vol. 1, Gaëtan Morin, Chicoutimi, Quebec, 1982
- 22 Ishimaru, A. 'Wave Propagation and Scattering in Random Media', Academic Press, New York, 1978
- 23 Schwarzschild, K. *Sitz. Ber. Preuss. Akad. Wiss. Berlin*, 1914, 1183
- 24 Maheu, B., Letoulouzan, N. and Gouesbet, G. *Appl. Opt.* 1984, **23**, 3353
- 25 Dangoux, R., Bissieux, C. and Egee, M. 'Thermal Transfer in Composite Materials', Eurotherm 4, Nancy, 1988